

## Mechanism of transonic aeroelastic instabilities via synchronization of coupled oscillators

Vasudevan, S.; Wang, Xuerui; De Breuker, R.

**Publication date**

2024

**Document Version**

Final published version

**Published in**

Aeroelasticity & Structural Dynamics in a Fast Changing World 17 – 21 June 2024, The Hague, The Netherlands

**Citation (APA)**

Vasudevan, S., Wang, X., & De Breuker, R. (2024). Mechanism of transonic aeroelastic instabilities via synchronization of coupled oscillators. In *Aeroelasticity & Structural Dynamics in a Fast Changing World 17 – 21 June 2024, The Hague, The Netherlands* Article IFASD 2024-164

**Important note**

To cite this publication, please use the final published version (if applicable). Please check the document version above.

**Copyright**

Other than for strictly personal use, it is not permitted to download, forward or distribute the text or part of it, without the consent of the author(s) and/or copyright holder(s), unless the work is under an open content license such as Creative Commons.

**Takedown policy**

Please contact us and provide details if you believe this document breaches copyrights. We will remove access to the work immediately and investigate your claim.

# MECHANISM OF TRANSONIC AEROELASTIC INSTABILITIES VIA SYNCHRONISATION OF COUPLED OSCILLATORS

Srikanth Vasudevan<sup>1</sup>, Xuerui Wang<sup>1</sup>, Roeland De Breuker<sup>1</sup>

<sup>1</sup>Delft University of Technology  
Kluyverweg 1, 2629HS Delft, The Netherlands  
S.Vasudevan@tudelft.nl

**Keywords:** Transonic buffet, coupled oscillators, beats, shock-dynamics

## Abstract:

This paper contributes towards the development of a reduced-order modelling methodology for nonlinear, unsteady aerodynamic loads for the active control of transonic aeroelastic flutter. To this end, a 1-DOF torsional NACA0012 airfoil is chosen as the test configuration. The aim is to develop the reduced-order model in nonlinear state-space form to be used in active control scenarios. Hence, a nonlinear coupled differential equation that captures the shock dynamics. The underlying hypothesis of this work is that, once these aerodynamic effects are included in the low-order model, the nonlinear trend in the flutter stability boundary, specifically in the transonic regime, will be predicted purely based on first principles, without the need for numerical or experimental corrections. In this work, we observe that the aeroelastic system could become prematurely unstable as soon as the aerodynamic flow field undergoes a Hopf bifurcation. For low amplitude airfoil pitching below a certain threshold, the aerostructural system is seen to exhibit a coupled oscillator behaviour that has an exact linear analytical formulation. The analytical formulation thus produces an accurate prediction whilst being orders of magnitude faster than the numerical simulation.

## 1 INTRODUCTION

With our continuous quest for optimality in aircraft design and performance through the lens of a sustainable aviation, aeroservoelastic (ASE) interactions have increased in recent years [1]. Generally, aeroelastic research involving load alleviation strategies can be broadly classified into active (using control surfaces and actuators) and passive (tailoring and optimizing composite lay-ups) methods. It is also realized that combining the effects of both active and passive load alleviation strategies can result in superior aeroelastic performance [2]. Concepts such as the VCCTEF [3] and Smart-X [4] are some examples of state-of-art distributed morphing technologies for active loads alleviation.

Within the field of aeroelasticity, the current focus of research is towards large aspect ratio wings such as the XHALE [5] and the Pazy wing [6]. In such configurations, the structural nonlinearities are of primary concern due to large deflections. Furthermore, they are often designed for low subsonic regimes and the aerodynamic panel codes provide sufficient accuracy under attached flow assumptions. However, most modern aircraft operate in the transonic regime, which necessitates the use of high-fidelity aerodynamic tools. In the last five years, there has been a substantial increase in interest towards transonic aeroelasticity at NASA [7–10]. More

specifically, the focus has been on building efficient reduced-order models for control law development [11–13]. Traditional linear ASE techniques implement reduction techniques due to the presence of large number of states. NASA has extended the use of these techniques to transonic aerodynamics [9–11]. However, it is observed that having the most efficient and accurate ROM for such nonlinearities is still an open question. Furthermore, most ROMs are built on steady aerodynamic GAFs from high-fidelity aerodynamics, and the unsteady effects are not considered. An erudite review of the need to model unsteady aerodynamics is provided by [14]

Traditionally, ASE modelling techniques are developed with the assumptions of linear superposition of eigenmodes. In practice, aeroservoelastic models for aircraft demonstrators such as the FLEXOP [15] and the NASA X56 [16] typically consist of a finite element (FE) structural model, a panel-based aerodynamic model such as the DLM/VLM. These coupled models are subjected to a reduction algorithm [17–19], following which controller synthesis is performed on the low-order state-space models. Beyond a certain regime, a bifurcation of the flow occurs due to the development of a supersonic region over the airfoil, leading to a normal shock. These numerical procedures are thus valid up to such a change in the flow behaviour, typically around Mach 0.7 - 0.8 [20].

Experimental research pertaining to oscillating structures in transonic windtunnels is quite sparse with Tijdeman [21] from the late 70s, McDevitt and Okuno [22] from the early 80s being referred to till date. The next two decades witnessed the emergence of several theories on the mechanism of self sustained flow oscillation and its potential contribution to the structural instability [20,23–26]. These have included the proposal of synchronisation and lock-in mechanisms often seen in coupled nonlinear systems. However, no low-order mathematical models exist that explain these phenomenon. More recently, several transonic wind tunnel campaigns focusing on controlling the shock motion have been undertaken [27, 28]. From a numerical perspective, in the last decade, several high-fidelity analyses have been performed [29–31]. However, these simulations are often infeasible for active control of such multi-physical systems. But, a given model often loses accuracy while reducing the fidelity of these numerical procedures.

To circumvent this issue, several instances of data-based numerical model correction procedures can be observed today: Ground Vibration Test (GVT) based finite-element (FE) model correction [15], wind-tunnel based Aerodynamic Influence Coefficient (AIC) matrix correction [15], look-up table based nonlinear model improvement [32] and CFD-based nonlinear reduced order models [33–35]. On the other hand, purely data-driven approaches exist [36], but often with limited mathematical basis and involve substantial hyper-parameter tuning to obtain an optimal fit [37, 38]. With such a setting, it is easy to overfit a model to a dataset with no physical significance and quite often requires a substantial amount of data for training [38, 39]. It is, therefore, evident that combining both physics-based and data-based simulation in a logical manner is the key to achieving accurate numerical predictions. An ideal middle ground then would be to identify a set of governing differential equations that forms a reduced order model of the Navier-Stokes equations, which can then be cast into a nonlinear state-space form. This way, we obtain a link to first principles; there is minimal data dependency and hence more interpretable.

This work contributes towards building such a nonlinear model order reduction framework to be used for active control of aeroelastic instabilities in the transonic regime. In this paper, we present the amplitude and frequency effects of prescribed structural oscillations on the buffeting frequencies. Furthermore, we present some preliminary results showing the prowess of linear

analytical models that can capture these complex nonlinear phenomenon.

This paper is structured as follows: Section 2 presents the methodology adopted to generate the results. Section 3 discusses various aspects of aero-structure interaction in the transonic regime such as the amplitude and frequency effects, the suppression of natural dynamics of the flow field, and finally the extent of linearity of the observed phenomenon. Section 4 presents the conclusions and future work.

## 2 METHODOLOGY

This section provides the numerical procedures and settings utilised to generate the results in this work. Section 2.1 presents the details on the high fidelity fluid-structure simulations. Section 2.2 presents the details of the low fidelity mathematical model that captures the dynamics of shock-structure interaction.

### 2.1 High-Fidelity Computational Domain Definition

In this work, ANSYS Fluent 24R2 was used for the 2D transonic flow simulations of NACA0012 airfoil. The simulation parameters are summarised in table 1. The simulation domain shown in figure 1 along with the mesh settings are adopted from [40]. We utilise the 1-equation Spalart Allaramas (SA) turbulence closure model to carry out the unsteady Reynolds Average Navier-Stokes (uRANS) simulations. In this paper, two simulation scenarios are presented:

- A transonic flow analysis around a static airfoil at Mach  $M = 0.80$  and  $\alpha = 4.0^\circ$ . This is to identify the self-sustained transonic buffet frequency.
- A prescribed airfoil pitching motion analysis with 2 amplitudes ( $\Delta\alpha = \pm 1^\circ, \pm 2^\circ$ ) and 4 frequencies ( $\omega_s = \{12, 16, 20, 24\}$  Hz). Here, both the amplitude effects and the frequency coupling effects are studied.

Table 1: CFD Simulation Settings [40].

<b>Property</b>	<b>Definition</b>
Bounding Box	$15X \times 10X$ ( $X$ is the airfoil chord)
Mesh Domain	Mapped face meshing with $5.53 \times 10^5$ nodes
Airfoil geometry	NACA0012, 1 m chord, $\alpha = 4.0^\circ$
Flow settings	Spalart Allaramas uRANS model, Mach $M = 0.80$

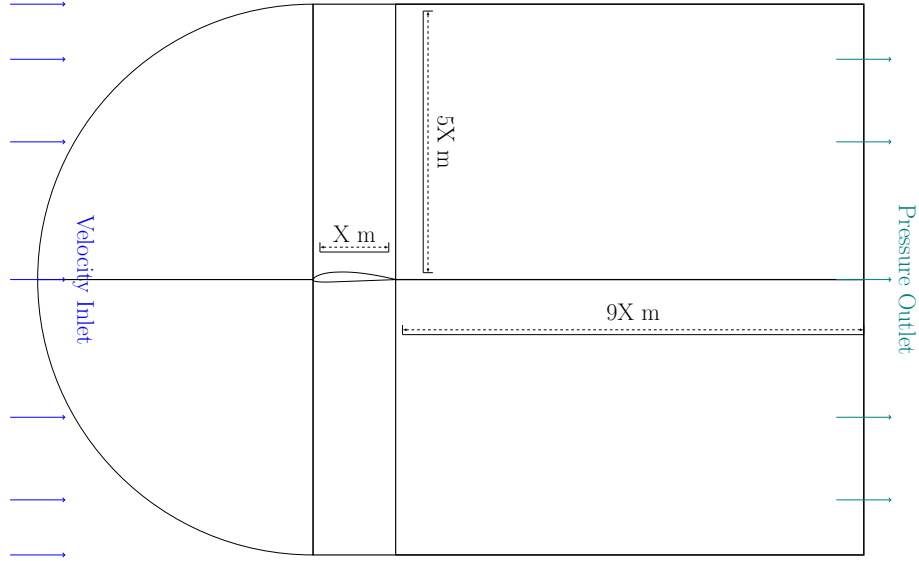


Figure 1: CFD Domain definition for structured meshing [40].

## 2.2 Analytical Coupled Oscillator

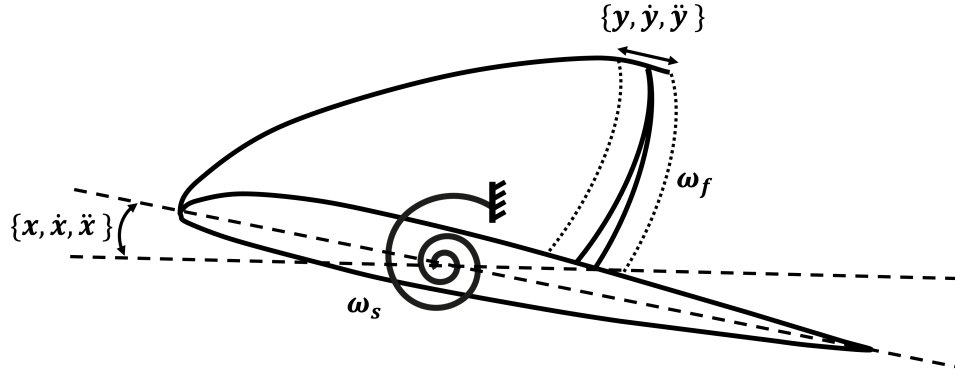


Figure 2: Transonic airfoil modelled as a coupled oscillator.

Consider the transonic airfoil modeled as a dynamical system of 2<sup>nd</sup> order shown in figure 2. A forced, coupled harmonic oscillator model can be defined as:

$$\begin{aligned}\ddot{x}(t) + \omega_s^2 x &= f(y(t), \omega_f, t) \\ \ddot{y}(t) + \omega_f^2 y &= g(x(t), \omega_s, t)\end{aligned}\quad (1)$$

where  $x, y$  are time-dependent states of the individual subsystems.  $\omega_s, \omega_f$  are the natural frequencies of the subsystems respectively.  $f, g$  in principle can take up any nonlinear form. But in general they are assumed to be functions of either  $\{x, y\}, \{\dot{x}, \dot{y}\}, \{\ddot{x}, \ddot{y}\}$ . Thereby making them displacement-coupling, velocity-coupling or acceleration-coupling respectively. In this work, a displacement-coupled model is used.

This analytical model is used in section 3.3 for verifying the high-fidelity simulations. Newmark-beta method [41] is used to integrate the given 2-system coupled equation iteratively in a staggered manner. For the sake of brevity and completeness, the staggered direct time integration scheme applied to the equation above is illustrated in figure 3.

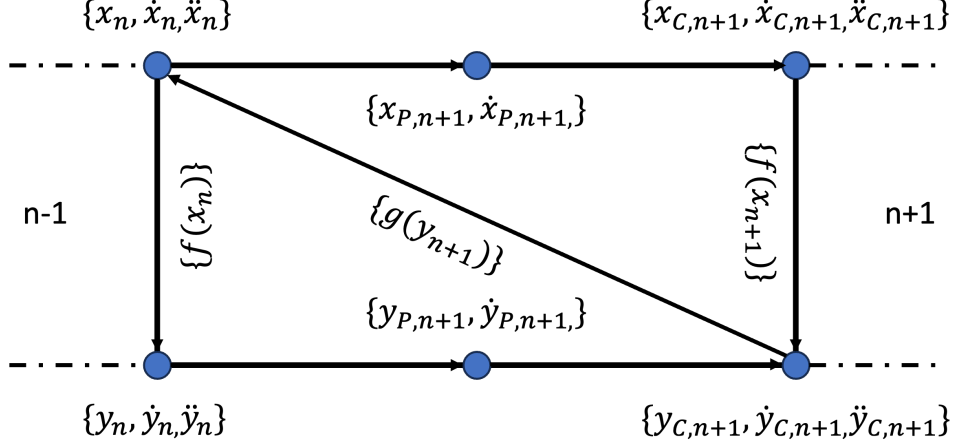


Figure 3: Staggered predictor-corrector time integration scheme.

### 3 RESULTS AND DISCUSSIONS

In order to study the influence of the structural motion on transonic buffet dynamics, the following 2D unsteady flow analysis was carried out. NACA0012 was chosen as the airfoil section. An unsteady RANS simulation with Spalart Allaramas (SA) turbulence closure model was used. The airfoil was subjected to 2 test cases: (a) Unsteady flow around the static airfoil at  $M = 0.80$ ,  $\alpha = 4.0^\circ$  and (b) Forced oscillations of the airfoil at 2 amplitudes, i.e.  $\Delta\alpha = \pm 1^\circ, \pm 2^\circ$  and 4 pitching frequencies, i.e.  $f = \{12, 16, 20, 24\}$  in Hz. The pitching motion was prescribed around the C.G. of the airfoil at half chord. In order to maintain spectral resolution to the required accuracy, the unsteady simulations were carried out for a total of  $t = 5s$ ,  $\Delta t = 0.001s$ .

#### 3.1 Amplitude effects of prescribed pitching frequencies

The first objective was to obtain a baseline unsteady flow regime that exhibits the self-sustained shock oscillations over the static NACA0012 airfoil. From a preliminary analysis,  $M = 0.80$ ,  $\alpha = 4.0^\circ$  was used to obtain this baseline unsteady flow field. In the results that follow, all temporal simulations are plotted for a 2-second time window after the initial transient responses have damped out.

Figure 4 illustrates the effect of low-amplitude structural oscillations, i.e.  $\Delta\alpha = \pm 1^\circ$ , on the unsteady lift coefficient. The subplots depict the effect of increasing the prescribed pitching oscillation frequency  $\omega_s$ , towards the buffet frequency  $\omega_f$ , sequentially. For a direct comparison, the purely unsteady shock motion around a static airfoil is plotted in red. Two significant effects can be observed here. Firstly, the aerodynamic buffet is directly influenced by the airfoil motion irrespective of the amplitude of the perturbation. Around a static airfoil, the unsteady lift fluctuation is a direct function of the characteristic buffet frequency. Next, as the airfoil is set into motion, the fluctuations in the lift coefficient is significantly impacted. The prescribed structural oscillations begin at half the buffet frequency. For this case shown in blue, the unsteady lift is seen to exhibit two distinct response cycles. One cycle having a higher response amplitude compared to the other. Thus indicating the existence of individual sub-system contributions. As the prescribed oscillation frequencies are further increased, the lift responses are seen to coalesce leading to the emergence of amplitude modulations with specific frequencies. This is similar to the phenomenon of beats in coupled oscillators. This crucial observation will be further investigated in section 3.3.

Figure 5 depicts the temporal variation of the pressure coefficient on the suction side of the airfoil. In order to provide a clear contrast in the effects observed, two prescribed oscillation test cases are compared to the transonic buffet around a static airfoil.

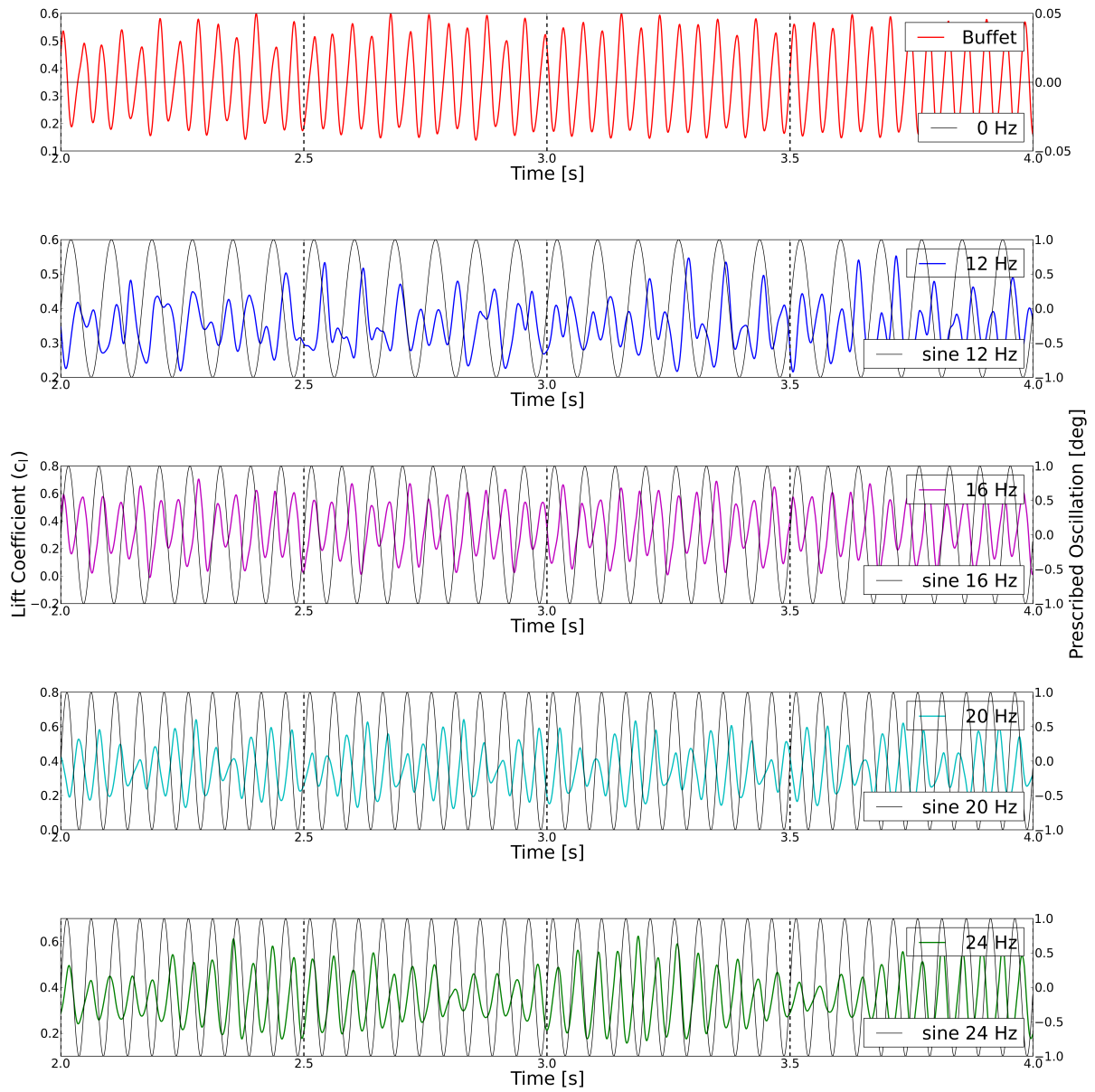


Figure 4: Temporal variation of lift coefficient for low amplitude pitching oscillations  $\Delta\alpha = \pm 1^\circ$ .

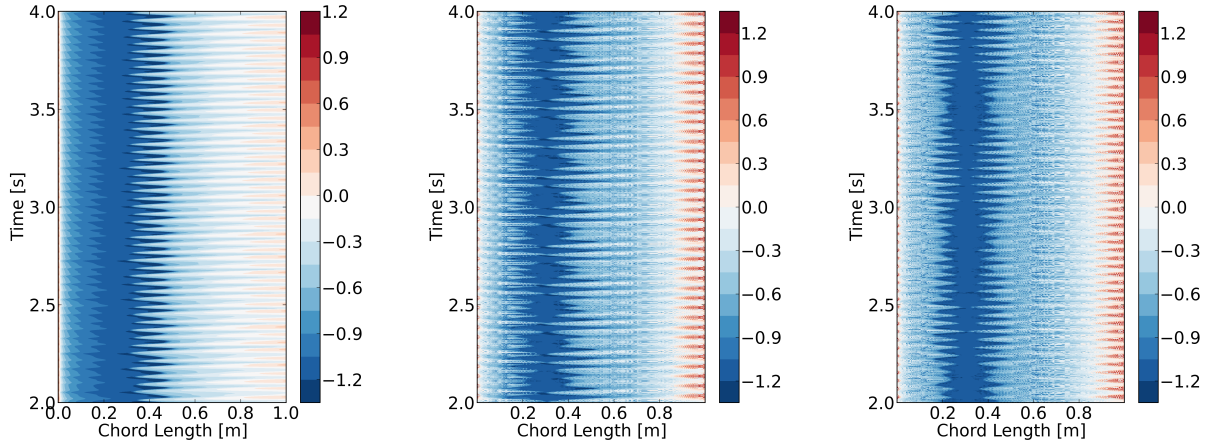


Figure 5: Temporal variation of suction-side pressure coefficient for  $\Delta\alpha = \pm 1^\circ$ : (Left)  $\omega_s = 0$  Hz. (Middle)  $\omega_s = 20$  Hz. (Right)  $\omega_s = 24$  Hz.

Firstly, in case of prescribed oscillations, the extent of supersonic region seems to be directly influenced by the local angle of attack. This is expected as there exists a minimum threshold angle of attack, approximately  $\alpha = 3.5^\circ$ , below which the shock disappears. In addition, by comparing the respective test cases in figures 4 and 5, a direct correlation can be made between the shock location and the coefficient of lift at any instance of time. Furthermore, as the prescribed pitching oscillation frequencies ( $\omega_s$ ) gets closer to the buffet frequency ( $\omega_f$ ), the aforementioned amplitude modulations are also observed in the temporal variation of the shock location as seen in figure 5. This confirms the influence of amplitude and frequency of the shock motion that could lead to the premature occurrence of aeroelastic instability in the transonic regime.

Next, figures 6 and 7 illustrate the effect of increasing the amplitude of the prescribed motion to  $\Delta\alpha = \pm 2^\circ$ . On a direct comparison to figure 4, the extent of amplitude modulation in 6 is smaller. In addition, the flow field is seen to have attained a constant phase lag irrespective of the frequency of oscillations. The amplitude modulation seen for the 16 Hz test case here is indicative of the existence of lock-in phenomenon observed in nonlinear coupled systems as described by Arnold Tongues [42]. Finally, close to the buffet frequency, the variation in lift coefficient is of constant amplitude, phase and frequency as seen for 24 Hz case in green. Thus, totally controlled by the structural motion. This is referred to as the suppression of natural dynamics of the flow, a phenomenon observed in the synchronization of coupled systems.

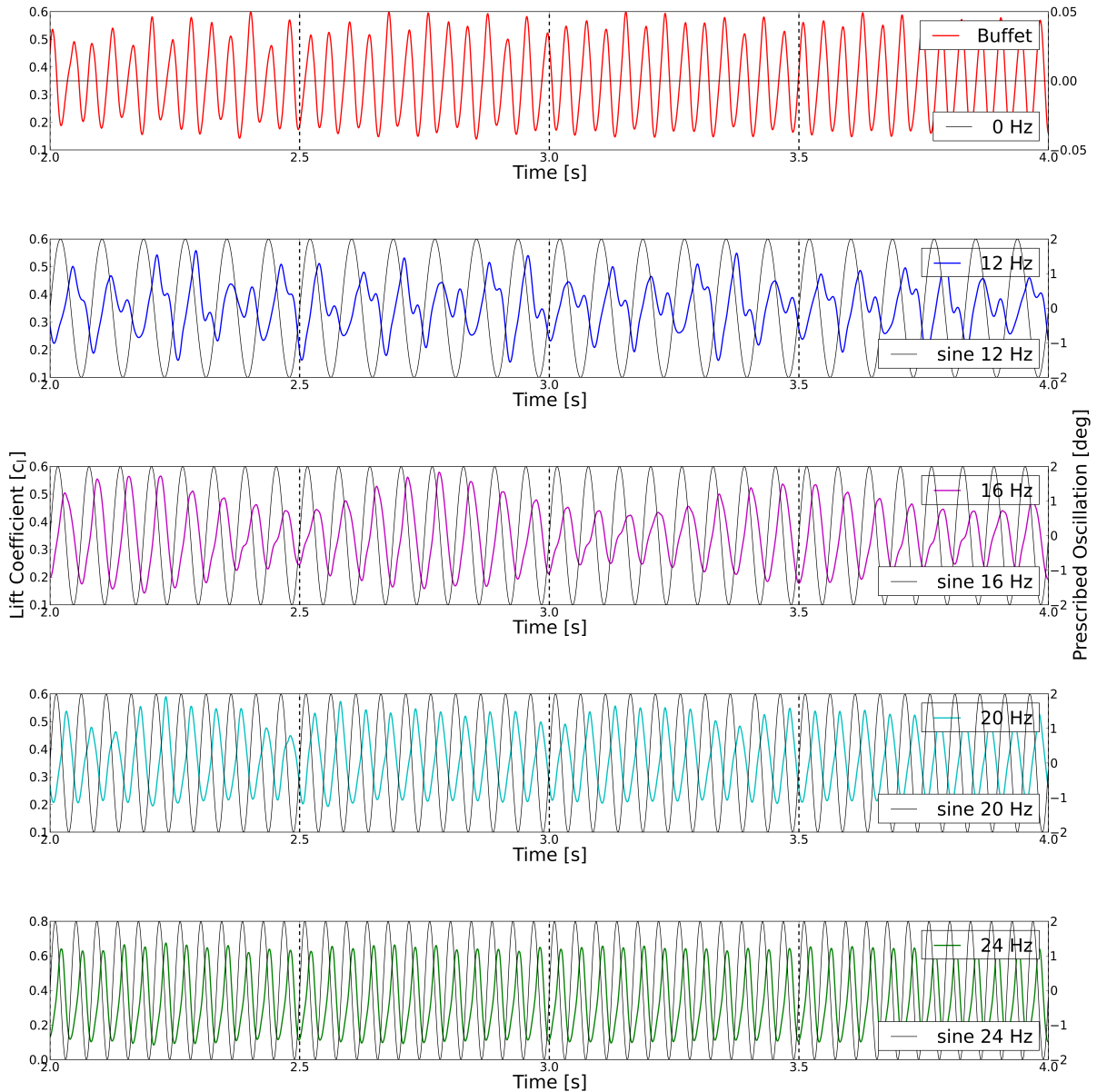


Figure 6: Temporal variation of lift coefficient for low amplitude pitching oscillations  $\Delta\alpha = \pm 2^\circ$ .

Similar to figure 5, figure 7 shows the pressure coefficient variation on the suction side of the airfoil for the high-amplitude test case. A constant amplitude shock motion is observed. This confirms that the flow field is now completely influenced by the structural motion. Summarising the amplitude variation analysis, there seems to be a threshold amplitude upto which the shock motion has an influence on the lift coefficient. Beyond this threshold, the shock dynamics is governed purely by the structural motion. This observation has a direct consequence to the assumptions in Theodorsen’s stability mechanism [43]. In the presence of an aerodynamic instability such as the transonic shock oscillation, a static airfoil can be forced into motion due to resonance, which can eventually lead to flutter as the threshold amplitude is crossed.

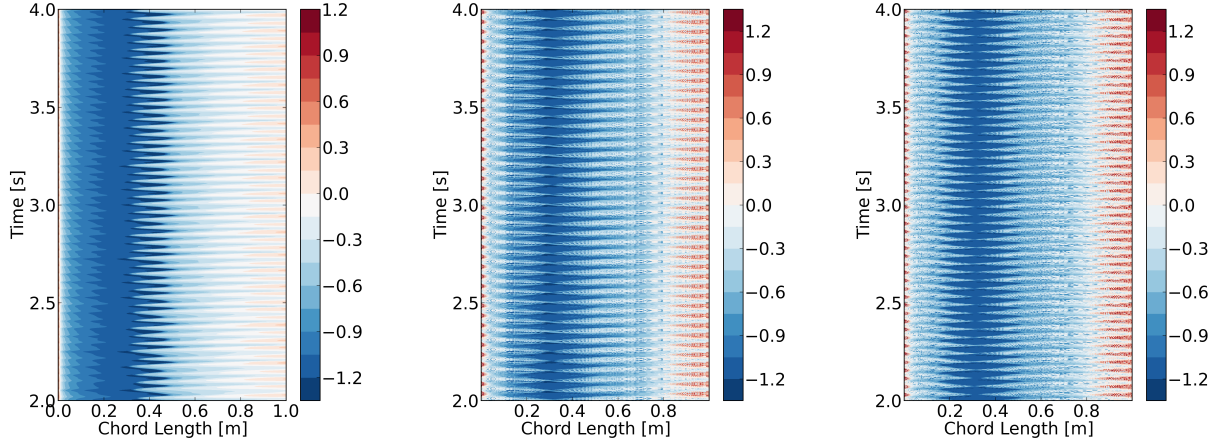


Figure 7: Temporal variation of suction-side pressure coefficient for  $\Delta\alpha = \pm 2^\circ$ : (Left)  $\omega_s = 0$  Hz. (Middle)  $\omega_s = 20$  Hz. (Right)  $\omega_s = 24$  Hz.

### 3.2 Frequency effects of prescribed pitching oscillations

Figure 8 shows the frequency spectrum of the lift coefficient fluctuations and hence, the pressure fluctuations in the flow field due to shock motion. Comparing the low amplitude responses with the high amplitude ones in figure 8, it is immediately noted that the spectral energy of the oscillating system is concentrated around the natural frequency of the transonic flow below a given threshold of amplitude. Figure 8 (left) clearly shows that all test cases have a dominant peak at the buffet frequency in addition to the peaks at their respective frequencies of oscillations. Also, the emergence of new peaks in the low frequency region again indicates the energy exchange leading to beats. Interestingly, as shown in figure 8 (right) these additional dominant peaks seem to disappear beyond the threshold amplitude. Thus confirming the influence of the structural motion on the buffet dynamics at high amplitudes.

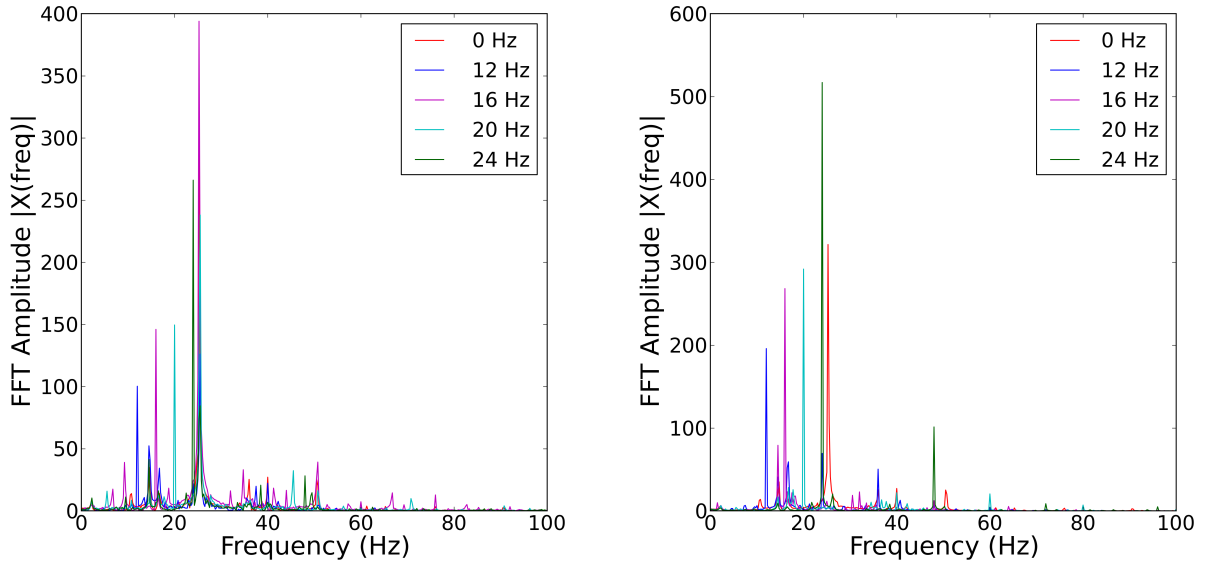


Figure 8: Frequency spectrum of the transonic flow field for prescribed pitching oscillations. (Left)  $\Delta\alpha = \pm 1^\circ$ , (Right)  $\Delta\alpha = \pm 2^\circ$ .

This brings us to our hypothesis on the mechanism involved in the transonic flutter: Considering a static airfoil submerged in a steady flow field. As the flow velocity increases and crosses

the critical Mach number, the flow bifurcates, giving rise to a stable periodic orbit and hence becoming unsteady. At this moment, the static airfoil is subjected to periodic forces at specific frequencies that could potentially cause amplified responses at its natural frequency. After this, as shown above, the transonic buffet follows the structural motion, feeding energy into the structure continuously. Thus forming a cascade of instabilities towards an early onset of aeroelastic flutter in this region, termed as "transonic dip".

### 3.3 Analytical Coupled Oscillator Model

It was observed that the low amplitude test case in section 3.1 was crucial in the energy exchange between the oscillating fluid and the stationary structure. In addition, the responses obtained as the prescribed structural frequencies approached the buffet frequency indicated the existence of a coupled oscillator behaviour. To verify this analogy, an analytical model was developed that uses a staggered, iterative direct numerical time integration scheme as described in 2.2. Figure 9 shows a direct comparison between the response of the analytical model and the high fidelity numerical model for similar operating conditions. These responses are analytically exact with a beating frequency  $\omega_{\text{beat}} = |\omega_1 - \omega_2|$ , indicating the possibility of analysing the inherently nonlinear system as a linear one for the low-amplitude case. It is imperative to note that the values obtained from the analytical model are normalised and centered around zero. This is due to the fact that the analytical equations used here describe an abstraction of two mass-normalised oscillators. Hence, the system frequencies and the beating phenomenon are of primary importance here.

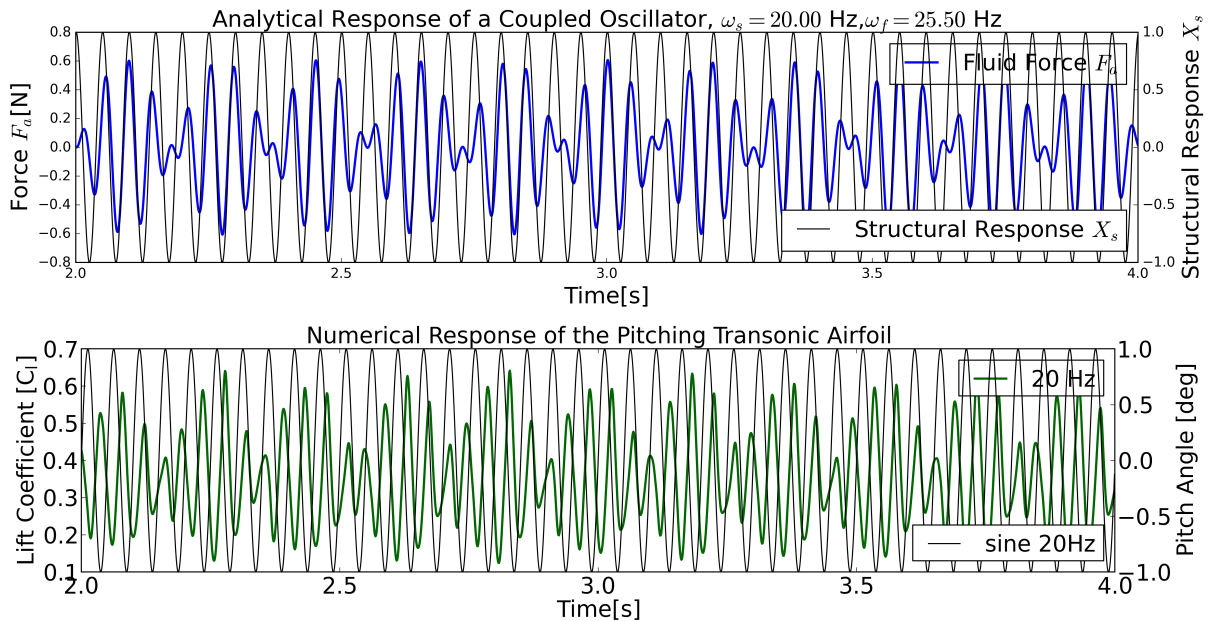


Figure 9: Comparison of analytical and numerical response of the coupled system: (Top) Linear coupled oscillator model with a  $\omega_{\text{beat}} = 5.50$  Hz. (Bottom) URANS (SA) model with prescribed oscillations having  $\omega_{\text{beat}} = 5.50$  Hz.

## 4 CONCLUSIONS

This work examines the nature of the transonic instability from the perspective of linear coupled oscillators. To this end, a high-fidelity fluid-structure model of NACA0012 was analysed for two main testcases: (a) Transonic aerodynamic buffet over a static airfoil and (b) Prescribed torsional motion of the airfoil subjected to transonic buffet. For the former, the op-

erating conditions used was  $M = 0.80$ ,  $\alpha = 4.0^\circ$ . For the latter, two studies were conducted. Firstly, two sinusoidal amplitudes were analysed for the amplitude effects, i.e.  $\Delta\alpha = \pm 1^\circ$  and  $\Delta\alpha = \pm 2^\circ$ . Next, the prescribed pitching motions consisted of sinusoidal frequencies ranging between  $\omega_s = 10$  Hz and  $\omega_s = 26$  Hz with  $\omega_f = 25.5$  Hz. Here, two major conclusions are drawn:

- The effect of increasing structural amplitudes leads to a suppression of natural dynamics of the flow. There exists a threshold of amplitude below which the oscillatory transonic flow influences the excitation of the structure via a coupled oscillatory motion. The phase of the flow field alternatively leads and lags that of the structure. Above this threshold, the flow field and hence the shock motion seems to consistently lag behind the structural motion and is only influenced by the structure.
- Within this crucial region below the aforementioned amplitude threshold, the response of the system can be physically explained by a linear coupled oscillator model with analytically derived exact values for beating frequencies. This indicates that the aeroelastic system can become unstable as soon as the flow becomes unsteady and oscillatory. The aeroelastic damping matrix need not be zero for the system to become unstable. The structure behaves as a forced oscillator in this region. Above this amplitude, aeroelastic model with a lagging aerodynamics becomes valid once again.

The results obtained in this work are crucial indicators for future work and pose several open questions. First, in order to completely prove the coupled oscillator analogy, the prescribed oscillation experiment must be extended to a fully coupled aero-structural simulations. Thus far, the results shown here are valid for a forced oscillatory system. Next, the amplitude effects, synchronisation effects and the suppression of natural dynamics are all topics of nonlinear systems and the current linear models will be extended to nonlinear differential equations for further analytical analysis of limit cycles. Finally, it is expected that such closed form analytical equations will be valid only for 2D simulations and extension of frameworks to 3D wings will require reliance on high-fidelity data for accurate models.

## 5 REFERENCES

- [1] Livne, E. (2018). Aircraft active flutter suppression: State of the art and technology maturation needs. *Journal of Aircraft*, 55(1), 410–452.
- [2] De Breuker, R., Binder, S., and Wildschek, A. (2018). Combined active and passive loads alleviation through aeroelastic tailoring and control surface/control system optimization. In *2018 AIAA Aerospace Sciences Meeting*. p. 0764.
- [3] Nguyen, N., Ting, E., and Lebofsky, S. (2015). Aeroelastic analysis of a flexible wing wind tunnel model with variable camber continuous trailing edge flap design. In *AIAA Science and Technology Forum and Exposition (SciTech 2015)*, ARC-E-DAA-TN20181.
- [4] Mkhoyan, T., Thakrar, N. R., De Breuker, R., et al. (2021). Design and development of a seamless smart morphing wing using distributed trailing edge camber morphing for active control. In *AIAA Scitech 2021 Forum*. p. 0477.
- [5] Cesnik, C. E., Senatore, P. J., Su, W., et al. (2012). X-hale: A very flexible unmanned aerial vehicle for nonlinear aeroelastic tests. *AIAA journal*, 50(12), 2820–2833.
- [6] Avin, O., Raveh, D. E., Drachinsky, A., et al. (2021). An experimental benchmark of a very flexiblewing. In *AIAA Scitech 2021 Forum*. p. 1709.

- [7] Bartels, R. E., Stanford, B., and Waite, J. (2019). Performance enhancement of the flexible transonic truss-braced wing aircraft using variable-camber continuous trailing-edge flaps. In *AIAA Aviation 2019 Forum*. p. 3160.
- [8] Jacobson, K., Stanford, B., Kiviaho, J. F., et al. (2021). Multiscale mesh adaptation for transonic aeroelastic flutter problems. In *AIAA Aviation 2021 Forum*. p. 2700.
- [9] Stanford, B. K. and Jacobson, K. E. (2021). Transonic aeroelastic modeling of the naca 0012 benchmark wing. *AIAA Journal*, 59(10), 4134–4143.
- [10] Stanford, B. and Jacobson, K. (2023). Transonic flutter dips of the agard 445.6 wing. In *AIAA SCITECH 2023 Forum*. p. 0589.
- [11] Waite, J., Stanford, B., Bartels, R. E., et al. (2019). Reduced order modeling for transonic aeroservoelastic control law development. In *AIAA Scitech 2019 Forum*. p. 1022.
- [12] Waite, J., Stanford, B., Bartels, R. E., et al. (2019). Active flutter suppression using reduced order modeling for transonic aeroservoelastic control law development. In *AIAA Aviation 2019 Forum*. p. 3025.
- [13] Nguyen, N. T., Fugate, J., Kaul, U. K., et al. (2019). Flutter analysis of the transonic truss-braced wing aircraft using transonic correction. In *AIAA SciTech 2019 Forum*. p. 0217.
- [14] Dowell, E. H. and Tang, D. (2002). Nonlinear aeroelasticity and unsteady aerodynamics. *AIAA journal*, 40(9), 1697–1707.
- [15] Meddaikar, Y. M., Dillinger, J., Klimmek, T., et al. (2019). Aircraft aeroservoelastic modelling of the flexop unmanned flying demonstrator. In *AIAA scitech 2019 forum*. p. 1815.
- [16] Ouellette, J. A. (2015). X-56a mutt: Aeroservoelastic modeling. Tech. rep.
- [17] Lieu, T., Farhat, C., and Lesoinne, M. (2005). Pod-based aeroelastic analysis of a complete f-16 configuration: Rom adaptation and demonstration. In *46th AIAA/ASME/ASCE/AHS/ASC structures, structural dynamics and materials conference*. p. 2295.
- [18] Amsallem, D., Zahr, M. J., and Farhat, C. (2012). Nonlinear model order reduction based on local reduced-order bases. *International Journal for Numerical Methods in Engineering*, 92(10), 891–916.
- [19] Amsallem, D., Farhat, C., and Lieu, T. (2013). Aeroelastic analysis of f-16 and f-18/a configurations using adapted cfd-based reduced-order models. In *48th AIAA/ASME/ASCE/AHS/ASC structures, structural dynamics, and materials conference*. p. 2364.
- [20] Dowell, E. H., Thomas, J. P., and Hall, K. C. (2004). Transonic limit cycle oscillation analysis using reduced order aerodynamic models. *Journal of Fluids and Structures*, 19(1), 17–27.
- [21] Tijdeman, H. (1977). Investigations of the transonic flow around oscillating airfoils. *NLR-TR 77090 U*.

- [22] McDevitt, J. B. and Okuno, A. F. (1985). Static and dynamic pressure measurements on a naca 0012 airfoil in the ames high reynolds number facility. Tech. rep.
- [23] Lee, B. (2001). Self-sustained shock oscillations on airfoils at transonic speeds. *Progress in Aerospace Sciences*, 37(2), 147–196.
- [24] Crouch, J., Garbaruk, A., Magidov, D., et al. (2008). Origin and structure of transonic buffet on airfoils. In *5th AIAA Theoretical Fluid Mechanics Conference*. p. 4233.
- [25] Jacquin, L., Molton, P., Deck, S., et al. (2009). Experimental study of shock oscillation over a transonic supercritical profile. *AIAA journal*, 47(9), 1985–1994.
- [26] van Rooij, A., Nitzsche, J., and Dwight, R. (2017). Prediction of aeroelastic limit-cycle oscillations based on harmonic forced-motion oscillations. *AIAA Journal*, 55(10), 3517–3529.
- [27] Korthäuer, T., Accorinti, A., Scharnowski, S., et al. (2023). Experimental investigation of transonic buffeting, frequency lock-in and their dependence on structural characteristics. *Journal of Fluids and Structures*, 122, 103975.
- [28] D’aguanno, A., Schrijer, F., and van Oudheusden, B. (2023). Investigation of three-dimensional shock control bumps for transonic buffet alleviation. *AIAA Journal*, 61(8), 3419–3431.
- [29] Raveh, D. E. and Dowell, E. H. (2014). Aeroelastic responses of elastically suspended airfoil systems in transonic buffeting flows. *AIAA journal*, 52(5), 926–934.
- [30] Iovnovich, M. and Raveh, D. E. (2015). Numerical study of shock buffet on three-dimensional wings. *AIAA Journal*, 53(2), 449–463.
- [31] Grossi, F., Braza, M., and Hoarau, Y. (2012). Delayed detached-eddy simulation of the transonic flow around a supercritical airfoil in the buffet regime. In *Progress in Hybrid RANS-LES Modelling: Papers Contributed to the 4th Symposium on Hybrid RANS-LES Methods, Beijing, China, September 2011*. Springer, pp. 369–378.
- [32] Lancelot, P. and De Breuker, R. (2021). Unsteady non-linear control surface modelling for aeroservoelastic applications. *Journal of Aeroelasticity and Structural Dynamics*, 8(1).
- [33] Lieu, T. and Farhat, C. (2007). Adaptation of aeroelastic reduced-order models and application to an f-16 configuration. *AIAA journal*, 45(6), 1244–1257.
- [34] Amsallem, D. and Farhat, C. (2008). Interpolation method for adapting reduced-order models and application to aeroelasticity. *AIAA journal*, 46(7), 1803–1813.
- [35] Carlberg, K., Bou-Mosleh, C., and Farhat, C. (2011). Efficient non-linear model reduction via a least-squares petrov–galerkin projection and compressive tensor approximations. *International Journal for numerical methods in engineering*, 86(2), 155–181.
- [36] Brunton, S. L., Proctor, J. L., and Kutz, J. N. (2016). Discovering governing equations from data by sparse identification of nonlinear dynamical systems. *Proceedings of the national academy of sciences*, 113(15), 3932–3937.

- [37] Champion, K., Lusch, B., Kutz, J. N., et al. (2019). Data-driven discovery of coordinates and governing equations. *Proceedings of the National Academy of Sciences*, 116(45), 22445–22451.
- [38] Swischuk, R., Mainini, L., Peherstorfer, B., et al. (2019). Projection-based model reduction: Formulations for physics-based machine learning. *Computers & Fluids*, 179, 704–717.
- [39] Bertrand, X., Tost, F., and Champagneux, S. (2019). Wing airfoil pressure calibration with deep learning. In *AIAA Aviation 2019 Forum*. p. 3066.
- [40] Vasudevan, S., De Breuker, R., and Wang, X. (2023). Manifold learning of nonlinear airfoil aerodynamics with dimensionality reduction. In *AIAA SCITECH 2023 Forum*. p. 1199.
- [41] Newmark, N. M. (1959). A method of computation for structural dynamics. *Journal of the engineering mechanics division*, 85(3), 67–94.
- [42] Pikovsky, A., Rosenblum, M., Kurths, J., et al. (2001). A universal concept in nonlinear sciences. *Self*, 2, 3.
- [43] Theodorsen, T. (1949). General theory of aerodynamic instability and the mechanism of flutter. Tech. Rep. TR-496, NACA.

## **COPYRIGHT STATEMENT**

The authors confirm that they, and/or their company or organisation, hold copyright on all of the original material included in this paper. The authors also confirm that they have obtained permission from the copyright holder of any third-party material included in this paper to publish it as part of their paper. The authors confirm that they give permission, or have obtained permission from the copyright holder of this paper, for the publication and public distribution of this paper as part of the IFASD 2024 proceedings or as individual off-prints from the proceedings.